

## State-Dependent Electron Delocalization Dynamics at the Solute-Solvent Interface: Soft-X-Ray Absorption Spectroscopy and *Ab Initio* Calculations

Sergey I. Bokarev,<sup>1,\*</sup> Marcus Dantz,<sup>2,3</sup> Edlira Suljoti,<sup>2,3</sup> Oliver Kühn,<sup>1</sup> and Emad F. Aziz<sup>2,3,\*</sup>

<sup>1</sup>*Institut für Physik, Universität Rostock, Universitätsplatz 3, D-18055 Rostock, Germany*

<sup>2</sup>*Joint Ultrafast Dynamics Lab in Solutions and at Interfaces (JULiQ), Helmholtz-Zentrum Berlin für Materialien und Energie, Albert-Einstein-Strasse 15, D-12489 Berlin, Germany*

<sup>3</sup>*Freie Universität Berlin, Fachbereich Physik, Arnimallee 14, D-14195 Berlin, Germany*

(Received 28 January 2013; published 20 August 2013)

Nonradiative decay channels in the *L*-edge fluorescence yield spectra from transition-metal–aqueous solutions give rise to spectral distortions with respect to x-ray transmission spectra. Their origin is unraveled here using partial and inverse partial fluorescence yields on the microjet combined with multireference *ab initio* electronic structure calculations. Comparing Fe<sup>2+</sup>, Fe<sup>3+</sup>, and Co<sup>2+</sup> systems we demonstrate and quantify unequivocally the state-dependent electron delocalization within the manifold of *d* orbitals as one origin of this observation.

DOI: [10.1103/PhysRevLett.111.083002](https://doi.org/10.1103/PhysRevLett.111.083002)

PACS numbers: 31.15.vj, 31.70.Dk, 32.80.Aa, 78.70.En

Interfaces between solvents and ionic species, where bond making and breaking takes place via valence molecular orbitals (MOs), are key to the function of materials from the molecular up to the nanoscale, and to the understanding of different chemical and biological processes [1,2]. Water is one of the major hosting solvents and plays a variety of roles at different levels of complexity, from molecules and cells to tissues and organisms [3–8]. A direct way to probe the local structure of this interface is to investigate the nature of the involved unoccupied MOs via atom specific core-level x-ray absorption (XA) spectroscopy [9,10]. In the case of transition metals (TM), excitation from and relaxation to the *L* edge addresses directly the empty valence and occupied *d* MOs, respectively. Here a new mechanism has been presented recently based on the observation of dips and peak reduction in the total fluorescence yield (TFY). These observations had been interpreted based on the electronic structure of the solute-solvent interface region [11,12]. This observation triggered a debate in the field of x-ray optics, because, in principle, these dips could be attributed to two effects: First, a change of the ratio of solvent background (i.e., from oxygen atoms) to the solute's metal *L*-edge emission [13–15], and, second, a charge delocalization between the metal *d* orbitals and the *p* orbitals of the solvent, which could be explained by electronic configuration mixing between ions and water molecules [15,16]. This would correspond to an ultrafast electron relaxation, with the electron dynamics occurring within the core-hole lifetime of a few femtoseconds. Achkar *et al.* and de Groot argued that only the first interpretation is reasonable [14,17], whereas Aziz *et al.*, on the basis of further investigations [12,16], concluded that both effects are coexisting [15]. It should be pointed out that the TFY reported in earlier studies [11,12] is not conclusive in this respect since it does not provide direct and quantitative information on the electronic

relaxation pathways of the *2p*-core excited TM ion [10,18]. Furthermore, the missing discrimination between the elastic and inelastic scattering in the TFY spectra adds more complication for understanding the main features. The partial fluorescence yield (PFY) measured for the metal center is more sensitive and avoids the solvent background [19]. Indeed, PFY represents integration over all emission channels at the metal *L* edge and allows not only for resolving metal emission but, in addition, discriminating between the resonant elastic and inelastic scattering which are both energy dependent. On the other side, the inverse partial fluorescence yield (IPFY) can be measured by inversion of the signal due to nonresonantly excited solvent atoms in the presence of the metal. This method for measuring the XA spectra has also been proven to be bulk sensitive and able to give absorption spectra free from optical artifacts (e.g., the saturation effect) [17,20,21]. Wernet *et al.* performed PFY measurements and argued that only the first interpretation (called optical effect) is valid [22]. However, their argument has been mostly based on semiempirical simulations of spectral line shapes. Furthermore, Lange *et al.* [23] have observed a reduction of bands at the *L*<sub>3</sub> edge of iron in the active centre of myoglobin upon ligation with different ligands, which cannot be attributed solely to the optical effect. In that study concentrations were kept constant far below the level of the optical effect discussed in Ref. [22].

For a quantitative interpretation of IPFY spectra a first-principles model is required, which can account for effects like solvent-induced electron-delocalization. Ligand field multiplet theory [24], widely used for interpretation of experimental results [10], being a semiempirical approach and treating the metal center in the field of the ligand's point charges, is not suitable for this purpose. Focusing on MO calculations of core-excitation spectra, (time-dependent) density functional theory (TDDFT) and nonempirical

multiplet DFT based configuration interaction methods, allowing for the treatment of metal ions in their environment explicitly, were successfully applied for predicting  $K$ -edge [25–29] and  $L$ -edge [30–33] XA spectra. But, in contrast to  $K$ -edge spectra, MO investigations of  $L$ -edge spectra are not well established. Here, an important point concerns the electronic multiconfigurational nature of the ground and excited states of TM complexes, which cannot be treated accurately by single-reference DFT methods.

The present work combines the power of the recently introduced IPFY and PFY measurements on a microjet in the soft-x-ray regime, with a first-principles based assignment. This allows drawing a comprehensive picture of the nature of MOs under the  $L$  edge of TMs and their role in electron delocalization. Specifically, the multireference restricted active space self-consistent field (RASSCF) method together with a state-interaction treatment of spin-orbit effects (RASSISO) is used to calculate the  $L$ -edge spectra of aqueous metal ions. On this basis a simple two-state model is formulated to explain the state-dependent electron delocalization dynamics, which leaves its fingerprints in fluorescence yield spectra. For illustration and validation of the method, different ions and oxidation states ( $\text{Fe}^{3+}$ ,  $\text{Fe}^{2+}$ , and  $\text{Co}^{2+}$ ) are considered that lead to specific spectral features and interpretations. The former two systems have been the subject of Refs. [11–16,22,34]. We have used a 1M concentration to compare with the previous analysis where the pH was close to neutral ( $\sim 6$ ) for  $\text{Fe}^{2+}$  and  $\text{Co}^{2+}$ , and 0.5 for  $\text{Fe}^{3+}$ .

Spectra were obtained using the newly developed high-resolution x-ray emission spectrometer with a Rowland circle and a liquid microjet as presented before in Refs. [19,20] (cf. Fig. S1a in the Supplemental Material [35]). The PFY spectra were recorded by setting the spectrometer to a given emission line and scanning the incident energy in the region of the TM  $L_{2,3}$  absorption edges ( $\text{Co}^{2+}$ ,  $\text{Fe}^{2+}$ , and  $\text{Fe}^{3+}$ ). For the IPFY, inversion of the nonresonantly excited oxygen  $K$ -edge fluorescence is used [19].

In the theoretical simulations,  $[M(\text{H}_2\text{O})_6]^{n+}$  ions ( $M = \text{Co}^{2+}$ ,  $\text{Fe}^{2+}$ , and  $\text{Fe}^{3+}$ ) as well as  $[\text{FeCl}(\text{H}_2\text{O})_5]^{2+}$  and  $[\text{FeCl}_2(\text{H}_2\text{O})_4]^+$  were calculated on the RASSCF level with the atomic natural orbital relativistically contracted valence triple zeta basis set [36,37]. The RASSISO treatment [38] included directly interacting states with  $\Delta S = 0, \pm 1$ . RASSCF and RASSI calculations were performed with MOLCAS 7.6 [39] (for details, see the Supplemental Material [35]).

In Fig. 1, experimental TFY, PFY, and IPFY spectra for the  $\text{Fe}^{3+}$  ion in water are presented. In comparison to the IPFY spectrum, which represents the absorption cross section free of artifacts [17,20,21], the PFY shows a lower pre-peak intensity (at  $\sim 708$  eV) and even a dip in case of the TFY, and a higher intensity for the  $L_2$  peak (721.0–726.5 eV). An analogous increase of  $L_2$  intensity in the PFY, if compared to IPFY, is shown in Fig. 2 for  $\text{Fe}^{2+}$  and

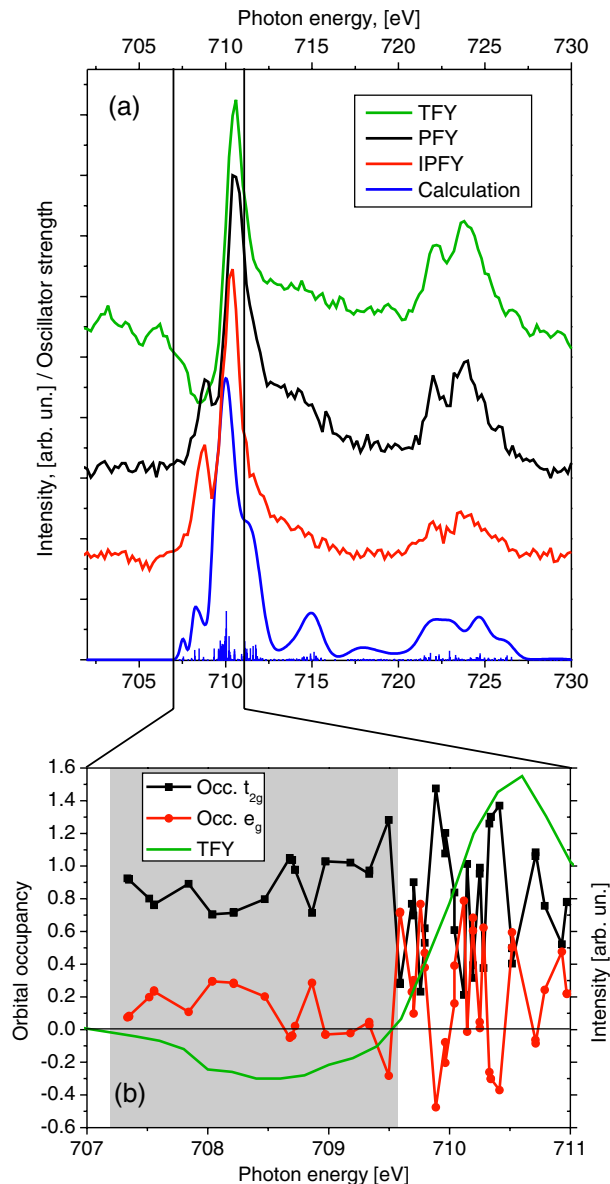


FIG. 1 (color online). (a) Experimental TFY, iron PFY, and oxygen IPFY spectra of a 1M  $\text{FeCl}_3$  solution in water as compared to the theoretical XA spectrum for  $[\text{Fe}(\text{H}_2\text{O})_6]^{3+}$  (from top). (b) Occupation numbers for  $t_{2g}$  and  $e_g$  3d orbitals of the metal ion correlated to the dip in the TFY spectrum. The shaded area marks the region where a core electron is predominantly excited to  $t_{2g}$  orbitals and the maximal distortion of the TFY occurs.

can be attributed to the Coster-Kronig effect for both ions [19]. The remaining parts of the spectra are similar for TFY, PFY, and IPFY. Figure 3 shows the  $L$ -edge transmission and TFY XA spectrum of a  $\text{CoCl}_2$  aqueous solution. Here we use the transmission XA spectrum as a reference for the true absorption cross section, thus proving that IPFY indeed is a method capable of measuring absorption free of artifacts [16,20]. The Co  $L_{1,\eta}$  PFY (corresponding to  $3s \rightarrow 2p$  transitions) is in good agreement with the transmission

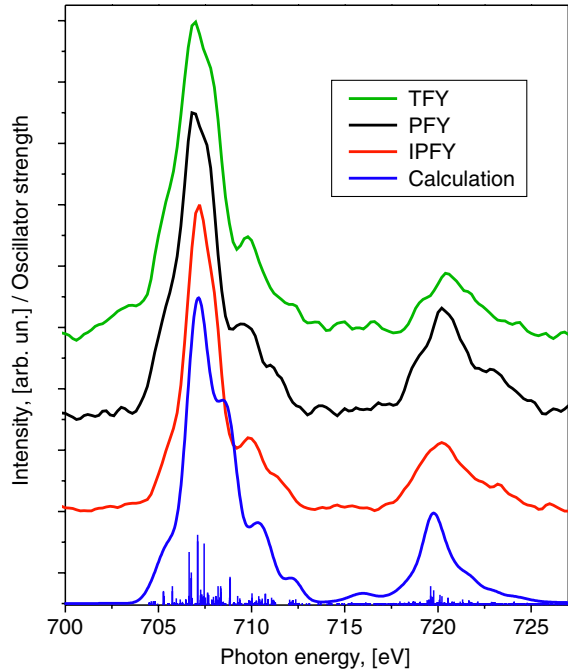


FIG. 2 (color online). Experimental TFY, iron PFY, and oxygen IPFY spectra of the 1M  $\text{FeCl}_2$  solution in water [19] as compared to the theoretical XA spectrum for  $[\text{Fe}(\text{H}_2\text{O})_6]^{2+}$  (from top).

spectrum after area normalization. Since it depends on the relaxation of the  $3s$  electron to the  $2p$  core hole, it gives unquenched photon-out events. Interestingly, the prepeak ( $\sim 775$  eV) in the  $\text{Co } L_{\alpha}$ , PFY spectrum ( $3d \rightarrow 2p$ ) is reduced in intensity relative to the  $\text{Co } L_{l,\eta}$  PFY and the transmission XA spectra. This fact could not be disentangled from the PFY data in Ref. [22] since it collects the total signal from  $L_l(3s \rightarrow 2p_{3/2})$ ,  $L_{\eta}(3s \rightarrow 2p_{1/2})$ ,  $L_{\alpha}(3d \rightarrow 2p_{3/2})$ , and  $L_{\beta}(3d \rightarrow 2p_{1/2})$  channels. The observation of lowered prepeak PFY intensities as well as dips in TFY for aqueous  $\text{Fe}^{3+}$  and  $\text{Co}^{2+}$  evidence a reduction of the fluorescence [20], e.g., due to electron delocalization into the solvent as discussed below.

This is supported by the previous partial-electron-yield study of Auger electrons [16], where a peak at 775 eV was reduced relative to the transmission spectrum. Hence, this mechanism is expected to decrease the nonradiative Auger rate as well. Both the optical effect and fluorescence reduction mentioned above result in a disappearance of the first peak at the  $L_3$  edge TFY of  $\text{Co}^{2+}$ .

The theoretical XA spectra are in fairly good agreement with transmission and PFY spectra for the investigated ions that validates the employed method (cf. Figs. 1–3). In fact, the present agreement seems to be superior to the level reached for  $\text{Cr}^{3+}$  in Ref. [22] employing a similar scheme. The analysis of the present results showed that mixing of states having different multiplicities is important to reproduce the experimental spectrum. In the  $\text{Co}^{2+}$  and  $\text{Fe}^{2+}$  spectra, the most intense transitions correspond to strongly allowed  $2p \rightarrow 3d(e_g) \Delta S = 0$  excitations. Remarkably, for

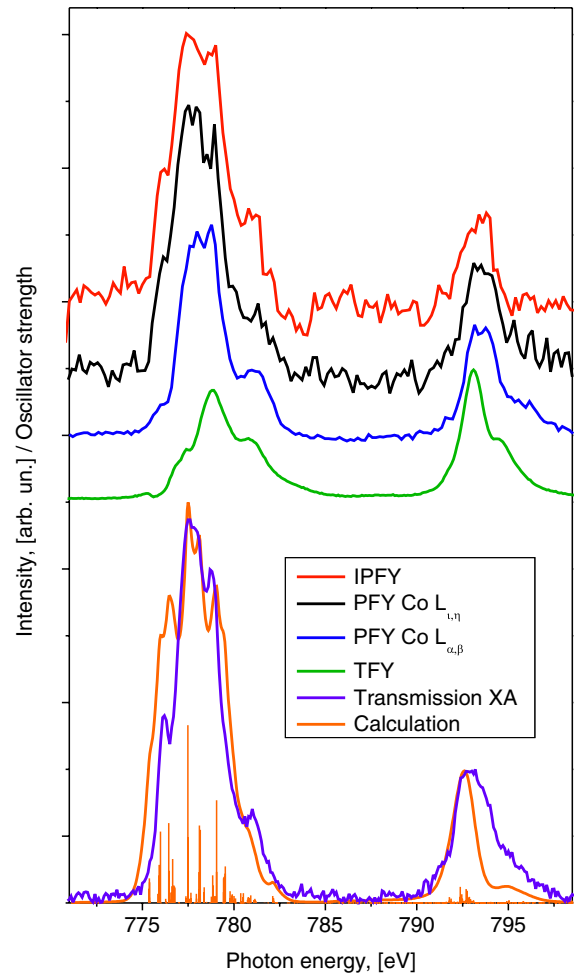


FIG. 3 (color online). Experimental oxygen IPFY and cobalt PFY  $L_{l,\eta}$  and  $L_{\alpha,\beta}$ , TFY, and transmission XA spectra of 1M  $\text{CoCl}_2$  solution in water [20] as compared to the theoretical XA spectrum for  $[\text{Co}(\text{H}_2\text{O})_6]^{2+}$  (from top).

$\text{Fe}^{3+}$  the XA spectrum is formed mainly by spin-forbidden sextet-quartet transitions though the most intense peaks are due to allowed sextet-sextet ones.

Most of the electronic states included in the calculations possess pronounced multiconfigurational character and are additionally mixed due to spin-orbit coupling. On the one hand, this emphasizes the importance of the  $n$ -particle character of the RASSCF wave function and gives an indication for a potential failure of TDDFT if applied to such problems. On the other hand, it hinders analysis and assignment of individual bands in terms of simple transitions between single particle MOs. However, for the low-energy side of the  $L_3$  edge the dominant character could be deduced quite clearly. Since this spectral region is the one that shows the most pronounced distortions in the TFY spectra, the following discussion will focus on establishing a relation between these distortions and the character of the underlying states. The latter will be classified as being either of  $e_g$  or  $t_{2g}$  character.

As illustrated in Fig. 1(b) and Supplemental Material Fig. S2, the low energy transitions correspond to predominant excitation of core-electrons to  $t_{2g}$  MOs. It should be emphasized that  $t_{2g}$  orbitals themselves do not extensively mix with water orbitals. But, through many-body effects the states in this region have contributions from configurations with a notable fraction of excited-core electron occupation on  $e_g$  orbitals mixed with solvent orbitals. If the core-electron is excited to  $e_g$  orbitals the extent of delocalization is notably higher and is now due to one-electron orbital mixing. This implies even larger charge delocalization for  $e_g$  dominated states than for  $t_{2g}$  dominated ones. Note that the presence of explicit water is vital for this picture to hold. Although a related point charge calculation yields a similar yet shifted spectrum, it cannot reproduce the nature of the MOs (see Fig. S3 in the Supplemental Material [35]).

In light of Fig. 1(b) and Fig. S2 in the Supplemental Material [35], the observed dips in TFY can be explained using the following simple two-state model. Let us assume that atomic  $2p$  orbitals of a metal ion ( $|2p\rangle$ ) are the initial states, whereas final states after electronic relaxation ( $t = \infty$ ) are the already mentioned  $|t_{2g}\rangle$  and  $|e_g\rangle$  states, where the core electron is excited to  $t_{2g}$  or  $e_g$   $3d$ -type orbitals of metal ions mixed with oxygen  $|2p_O\rangle$  states

$$|t_{2g}\rangle = C_{3d}^{t_{2g}}(t = \infty)|3d_{t_{2g}}\rangle + C_{2p_O}^{t_{2g}}(t = \infty)|2p_O\rangle.$$

$$|e_g\rangle = C_{3d}^{e_g}(t = \infty)|3d_{e_g}\rangle + C_{2p_O}^{e_g}(t = \infty)|2p_O\rangle.$$

Note that for the cases considered we have  $C_{2p_O}^{t_{2g}}(t = \infty) < C_{2p_O}^{e_g}(t = \infty)$ . The excitation at time  $t = 0$  occurs via the local atomic transition dipole operator

$$\hat{D} = d_{2p \rightarrow t_{2g}}|3d_{t_{2g}}\rangle\langle 2p| + d_{2p \rightarrow e_g}|3d_{e_g}\rangle\langle 2p| + \text{H.c.}$$

The nonstationary wave function after excitation at time  $t = 0$  depending on the wavelength reads

$$|\Psi(t=0)\rangle = \hat{D}|2p\rangle = C_{3d}^{t_{2g}}(t=0)|3d_{t_{2g}}\rangle \text{ or } C_{3d}^{e_g}(t=0)|3d_{e_g}\rangle,$$

where  $C_{3d}^{t_{2g}}(t=0) \propto d_{2p \rightarrow t_{2g}}$  and  $C_{3d}^{e_g}(t=0) \propto d_{2p \rightarrow e_g}$ , i.e., only the local  $3d$  component [ $C_{2p_O}^{e_g}(t=0) = 0$  and  $C_{2p_O}^{t_{2g}}(t=0) = 0$ ] of the delocalized ground state MOs is excited. The time evolution of this nonstationary state is that of simple two level system with the Hamiltonian

$$H = \begin{pmatrix} E_{3d} & V \\ V & E_{2p_O} \end{pmatrix}.$$

It proceeds as a decrease of metal  $3d$  contributions ( $C_{3d}^{e_g}$  and  $C_{3d}^{t_{2g}}$ ) with simultaneous increase of the water  $2p$  contributions ( $C_{2p_O}^{e_g}$  and  $C_{2p_O}^{t_{2g}}$ ) towards a delocalized stationary state. If  $E_{3d} - E_{2p_O}$  and  $V$  differ not much for both types of  $d$  orbitals, the rates of this delocalization are similar. An

essential point is the difference in the emission life times determined by the absolute square of  $d_{2p \rightarrow t_{2g}} C_{3d}^{t_{2g}}(t)$  or  $d_{2p \rightarrow e_g} C_{3d}^{e_g}(t)$ . Here, for the most intense transitions  $d_{2p \rightarrow e_g} / d_{2p \rightarrow t_{2g}} \approx 10$  holds according to the RASSCF and RASSISO calculations. Two cases can be distinguished (a) The excited state has dominant  $t_{2g}$  character and the life time is relatively long due to the smallness of  $d_{2p \rightarrow t_{2g}}$ . This means that the electron delocalization to water can occur completely and the fluorescence intensity decreases. (b) The excited state has dominant  $e_g$  character what implies shorter life times and incomplete electron relaxation. As a result fluorescence intensity is not much affected. Thus, based on the above picture, the ultrafast electron dynamics and the associated fluorescence spectra depend on the initial state selected by the wavelength of excitation. It is important to emphasize that we consider electron delocalization to water rather than “real” metal-to-water charge transfer leading to an  $n + 1$  times charged metal ion and a solvated electron.

Returning to the experimental data and taking into account that (a) except for prepeak the TFY, PFY, and IPFY spectra are similar and (b) both  $\text{Fe}^{2+}$  and  $\text{Fe}^{3+}$  have the same concentration in water and the background effect for both cases is similar, the observation of reduced prepeak intensities and dips shows the existence of the nonradiative relaxation at the  $L$  edge of aqueous  $\text{Fe}^{3+}$ . This conclusion is supported by XA studies on the solvent  $K$  edge ( $K$  edge of waters’ oxygen) [34],  $L$  edge XA spectra of TM complexes [12], and photoelectron spectroscopy [16].

In case of aqueous  $\text{Fe}^{3+}$  ion, there is an extended region 707.0–709.5 eV where the excited electron occupies dominantly  $t_{2g}$  states [shaded area in Fig. 1(b)] and the decrease in fluorescence intensity leads to dips below the background level. Note, that the same holds true for  $[\text{FeCl}(\text{H}_2\text{O})_5]^{2+}$  and  $[\text{FeCl}_2(\text{H}_2\text{O})_4]^{2+}$  which, together with  $[\text{Fe}(\text{H}_2\text{O})_6]^{3+}$ , are the main species in solution under experimental conditions (see Figs. S4 and S5 in the Supplemental Material [35]). For  $\text{Fe}^{2+}$  and  $\text{Co}^{2+}$ ,  $e_g$  occupation starts to dominate at the low energy edge and the fluorescence is less affected (see Fig. S2 [35]). If we now take into account that in case of  $\text{Fe}^{2+}$  the orbital mixing is less pronounced [ $C_{2p_O}^{t_{2g}}(t = \infty)$  and  $C_{2p_O}^{e_g}(t = \infty)$  are calculated to be a factor of three smaller than for  $\text{Fe}^{3+}$ ], this indeed supports the experimental observation where the dip in TFY is strongest for  $\text{Fe}^{3+}$ , weaker for  $\text{Co}^{2+}$ , and almost negligible for  $\text{Fe}^{2+}$ . Note, that  $\text{Fe}^{2+}$  in this respect behaves similar to  $\text{Cr}^{3+}$  studied recently [22]. Thus, the extent of delocalization of excited core electron on solvent molecules through single-particle (orbital mixing) and many-particle (electron correlation) effects observed in theoretical calculations correlates with the extent of TFY distortion in the experiments (this cannot be captured by a point charge model; see Fig. S3 [35]). The differences in radiative lifetimes for different core-excited states explain why the electron delocalization is

state dependent and spectral distortions in PFY and TFY relative to the true absorption cross section are observed only for the prepeak region.

Summarizing, the combination of *ab initio* multiconfigurational calculations (RASSCF and RASSISO) with recently developed high-resolution PFY and IPFY for the study of *L*-edge XA spectra of TM aqueous ions demonstrated that beside the well-known background effect (x-ray optical effect), electron delocalization across the metal-solvent interface can be, depending on the metal species, responsible for the TFY and PFY spectral distortions. For Fe<sup>3+</sup> and partially also for Co<sup>2+</sup> this behavior depends on the nature of the excited state and the ratio between its radiative life time and electronic relaxation time. Here the fluorescence dips correspond to the predominant *t*<sub>2g</sub> occupation of the core electron. Although the *e*<sub>g</sub> states of the *d* orbitals are more strongly mixed with the solvent molecular orbitals, because of longer life times, *t*<sub>2g</sub> states lead to a more pronounced electron delocalization into the water solvation shell.

This work was supported by the Helmholtz-Gemeinschaft via the VH-NG-635 grant (E. F. A.) and the European Research Council starting Grant No. 279344 (E. F. A.).

\*Corresponding authors.

Sergey.Bokarev@uni-rostock.de

Emad.Aziz@fu-berlin.de

- [1] J. J. R. Fraústo da Silva and R. J. P. Williams, *The Biological Chemistry of the Elements: The Inorganic Chemistry of Life* (Oxford University Press, Oxford, 1991).
- [2] D. Wöhrle and A. D. Pomogailo, *Metal Complexes and Metals in Macromolecules: Synthesis, Structure and Properties* (Wiley-VCH, Berlin, 2003).
- [3] J. H. Guo, Y. Luo, A. Augustsson, J.-E. Rubensson, C. Sätze, H. Ågren, H. Siegbahn, and J. Nordgren, *Phys. Rev. Lett.* **89**, 137402 (2002).
- [4] U. Bergmann, D. Nordlund, Ph. Wernet, M. Odelius, L. G. M. Pettersson, and A. Nilsson, *Phys. Rev. B* **76**, 024202 (2007).
- [5] K. M. Lange, M. Soldatov, R. Golnak, M. Gotz, N. Engel, R. Könnecke, J.-E. Rubensson, and E. F. Aziz, *Phys. Rev. B* **85**, 155104 (2012).
- [6] *Water and Life: The Unique Properties of H<sub>2</sub>O*, edited by R. M. Lynden-Bell, S. C. Morris, J. D. Barrow, J. L. Finney, and C. L. Harper Jr. (CRC Press, Boca Raton, 2010).
- [7] D. S. Goodsell, *The Machinery of Life* (Springer, New York, 1993).
- [8] P. Ball, *Chem. Rev.* **108**, 74 (2008).
- [9] J. Stöhr, *NEXAFS Spectroscopy* (Springer-Verlag, Berlin, 1992).
- [10] F. de Groot and A. Kotani, *Core Level Spectroscopy of Solids* (CRC Press, Boca Raton, 2008).
- [11] E. F. Aziz, M. H. Rittmann-Frank, K. M. Lange, S. Bonhommeau, and M. Chergui, *Nat. Chem.* **2**, 853 (2010).
- [12] M. Bauer, T. Stalinski, and E. F. Aziz, *ChemPhysChem* **12**, 2088 (2011).
- [13] T. Z. Regier, A. J. Achkar, D. Peak, J. S. Tse, and D. G. Hawthorn, *Nat. Chem.* **4**, 765 (2012).
- [14] F. M. F. de Groot, *Nat. Chem.* **4**, 766 (2012).
- [15] E. F. Aziz, K. M. Lange, S. Bonhommeau, and M. Chergui, *Nat. Chem.* **4**, 767 (2012).
- [16] R. Seidel *et al.*, *J. Am. Chem. Soc.* **134**, 1600 (2012).
- [17] A. J. Achkar, T. Z. Regier, H. Wadati, Y.-J. Kim, H. Zhang, and D. G. Hawthorn, *Phys. Rev. B* **83**, 081106 (2011).
- [18] F. de Groot, *Coord. Chem. Rev.* **249**, 31 (2005).
- [19] M. D. Gotz, M. A. Soldatov, K. M. Lange, N. Engel, R. Golnak, R. Könnecke, K. Atak, W. Eberhardt, and E. F. Aziz, *J. Phys. Chem. Lett.* **3**, 1619 (2012).
- [20] M. A. Soldatov, K. M. Lange, M. D. Gotz, N. Engel, R. Golnak, A. Kothe, and E. F. Aziz, *Chem. Phys. Lett.* **546**, 164 (2012).
- [21] A. J. Achkar, T. Z. Regier, E. J. Monkman, K. M. Shen, and D. G. Hawthorn, *Sci. Rep.* **1**, 182 (2011).
- [22] P. Wernet, K. Kunnus, S. Schreck, W. Quevedo, R. Kurian, S. Techert, F. M. F. de Groot, M. Odelius, and A. Föhlisch, *J. Phys. Chem. Lett.* **3**, 3448 (2012).
- [23] K. M. Lange, R. Golnak, S. Bonhommeau, and E. F. Aziz, *Chem. Commun. (Cambridge)* **49**, 4163 (2013).
- [24] B. T. Thole, G. van der Laan, J. Fuggle, G. Sawatzky, R. Karnatak, and J.-M. Esteva, *Phys. Rev. B* **32**, 5107 (1985).
- [25] M. Stener, G. Fronzoni, and M. de Simone, *Chem. Phys. Lett.* **373**, 115 (2003).
- [26] R. G. Wilks, J. B. MacNaughton, H.-B. Kraatz, T. Regier, and A. Moewes, *J. Phys. Chem. B* **110**, 5955 (2006).
- [27] S. DeBeer George, T. Petrenko, and F. Neese, *J. Phys. Chem. A* **112**, 12936 (2008).
- [28] W. Liang, S. A. Fischer, M. J. Frisch, and X. Li, *J. Chem. Theory Comput.* **7**, 3540 (2011).
- [29] N. A. Besley and D. Robinson, *Faraday Discuss.* **148**, 55 (2011).
- [30] L. G. M. Pettersson, T. Hatsui, and N. Kosugi, *Chem. Phys. Lett.* **311**, 299 (1999).
- [31] G. Fronzoni, M. Stener, P. Decleva, F. Wang, T. Ziegler, E. van Lenthe, and E. J. Baerends, *Chem. Phys. Lett.* **416**, 56 (2005).
- [32] M. Casarin, P. Finetti, A. Vittadini, F. Wang, and T. Ziegler, *J. Phys. Chem. A* **111**, 5270 (2007).
- [33] H. Ikeno, T. Mizoguchi, and I. Tanaka, *Phys. Rev. B* **83**, 155107 (2011).
- [34] L.-Å. Näslund, M. Cavalleri, H. Ogasawara, A. Nilsson, L. G. M. Pettersson, P. Wernet, D. C. Edwards, M. Sandström, and S. Myneni, *J. Phys. Chem. A* **107**, 6869 (2003).
- [35] See Supplemental Material at <http://link.aps.org/supplemental/10.1103/PhysRevLett.111.083002> for details on experimental setup and additional analysis of *ab initio* results.
- [36] B. O. Roos, R. Lindh, P.-Å. Malmqvist, V. Veryazov, and P.-O. Widmark, *J. Phys. Chem. A* **108**, 2851 (2004).
- [37] B. O. Roos, R. Lindh, P.-Å. Malmqvist, V. Veryazov, and P.-O. Widmark, *J. Phys. Chem. A* **109**, 6575 (2005).
- [38] P.-Å. Malmqvist, B. O. Roos, and B. Schimmelpfennig, *Chem. Phys. Lett.* **357**, 230 (2002).
- [39] G. Karlström *et al.*, *Comput. Mater. Sci.* **28**, 222 (2003).